Stability of a Droplet Vaporizing in a Hot Atmosphere

F.J. Higuera* and A. Liñán†
Universidad Politécnica de Madrid, Madrid, Spain

Abstract

A linearized stability analysis is carried out for an evaporating liquid droplet in a hot atmosphere with a view to understand the stabilizing effects of surface tension together with the unstabilizing effects of expansion, due to the phase change, and of the motion in the liquid induced by tangential viscous stress on the interface. The analysis is carried out for both small and order-one gas Reynolds number based on the unperturbed Stefan flow. Two different surfaces bound the stability domain; on one of them, the growth rate of the perturbations is imaginary and on the other, vanishes.

Introduction

The subject of quasisteady droplet vaporization has received considerable attention in the literature. Under very general conditions, the mass vaporization rate per unit area of the interface of a droplet evaporating in a stagnant hot atmosphere is proportional to the inverse of the droplet radius. Therefore, the area of the interface, or the square of its diameter, decreases at a constant rate. This behavior was first observed by Sreznersky in 1882, and its explanation, given by Langmuir in 1918, is based on the fact that the mass flux is directly related to the heat flux coming to the interface from the gas, which is proportional to the inverse of the droplet radius. Later the "d-square law" was found to hold true for the consumption of a droplet of fuel burning in an oxidizing atmosphere.

The "d-square law" results from assuming that the droplet temperature is constant equal to the boiling temperature, so that no heat is transferred to the interior of the droplet. In addition the quasisteady assumption is used for

Presented at the 10th ICDERS, Berkeley, California, August 4-9, 1985.

*Assistant Professor, Department of Fluid Mechanics, E.T.S.I. Aeronáuticos.

†Professor, Department of Fluid Mechanics, E.T.S.I.Aeronáuticos.

the gas phase. These assumptions have not been used in more refined analyses, see for example the review by Sirignano (1983), but the literature on the stability of the droplet vaporization process is very scarce.

When describing the liquid oscillations, one can take advantage of the fact that the gas-to-liquid density and viscosity ratios are small to neglect, in first approximation, the effect of the gas phase stresses on the droplet surface. This has been done in analysing the free oscillations of droplets and bubbles, first considered, in a way or another, by Kelvin (1890) and Rayleigh (1894) for the inviscid case; they found and undamped oscillatory motion. However viscous effects lead to the damping of these oscillations as it as been shown first by Lamb (1932), who considered the small viscosity case. The more viscous cases were treated by Chandrasekhar (1959) and Reid (1960). An attempt to generalize the results of the small viscosity case to account for the possibly destabilizing effect of the vaporization, when this can be considered as a small perturbation, is presently under study and will be published elsewhere.

In this paper we shall analyze another aspect of the linear stability of the vaporization of a droplet in a hot atmosphere, involved with a slow response of the system associated with the nonuniform temperature distribution within the droplet, found in the initial stages of the droplet vaporization. Small perturbations in the local vaporization rate can induce instabilities which disappear altogether when the liquid temperature distribution becomes uniform.

Instabilities of planar vaporizing interfaces, associated with nonuniform temperature distributions within the liquid have been described in the literature. For example, Palmer (1976) analyzed the stability of the vaporization of a superheated liquid, pointing out the role of the shear stress exerted on the liquid surface by the gas as a possibly relevant destabilizing factor, among others. The effect on the interface of pressure perturbations in the gas due to changes in the local vaporization rate and due to the motion of the gas was pointed out by Hickman (1952; 1972) for this same problem, and similar effects had been found before by Landau (1944) for a flame propagating in a combustible gas mixture. In all these cases of unperturbed planar interfaces the viscosity does not play an important role in the determination of the velocity and pressure perturbations. Transport effects are, however, essential in the droplet vaporization problem, because the heat has to arrive at the interface by conduction against the radial outward flow induced by the vaporization. The pressure per-

turbations now take a different form; however, they still have an important effect on the stability when the deformation of the interface is to be accounted for in the analysis.

Here the limit of small gas-to-liquid density and viscosity ratios will be used. At the interface, we assume a local thermodynamic equilibrium condition, leading to the Clausius-Clapeyron relation, but, in many cases, when vaporization occurs, the interface temperature is almost constant, close to the boiling temperature, because the ratio cT_b/L of the specific internal energy at the boiling temperature to the specific latent heat is moderately small.

We begin by describing the spherically symmetrical, unperturbed, vaporization process that in the limiting case indicated above includes three stages.

In a first stage the droplet is heated without significant vaporization until the surface temperature reaches a value close to the boiling temperature T_b; in this stage the stability analyses for a nonvaporizing droplet are applicable.

In a second stage the surface temperature is close to T_b, but a fraction of the heat reaching the droplet surface is transported to the interior of the droplet to uniformize the temperature distribution. The vaporization mass flux increases during the second stage from a negligible value to the quasisteady value corresponding to the third stage, that cover most of the lifetime of the droplet, when the liquid temperature is nearly uniform.

In the stability analysis two time scales appear. There is a fast response associated to the motion in the gas phase and a slow one associated to the liquid. When trying to describe the instabilities associated with the fast response, we found that, within the framework of the present model, the effects of the perturbations in the heat flux entering the droplet during the second heating-vaporization stage are negligible, so that this analysis is essentially the same for the second and third stages. It turns out that there are not instabilities associated to the fast response of the gas, and for this reason the stability analysis presented in this paper is restricted only to the slow time scale. The quasisteady state approximation is used in the analysis that follows, because the times involved are long compared with the gas-phase response time.

Two main parameters are found to control the stability properties during the heating-vaporization period. One is the Reynolds number β, based on the droplet radius and the typical gas phase vaporization flow; the other parameter,

Σ, is the ratio of the pressure jump due to surface tension and the typical gas viscous stresses.

The analysis is first carried out for low ambient temperatures, when the vaporization rate is small enough to make the Reynolds number small, and for large values of Σ, so that the deformations of the interface can be neglected: The motion induced in the liquid by the viscous drag of the gas through the interface has a destabilizing effect, opposite to that of the motion induced by changes in surface tension, due to interface temperature perturbations, which is stabilizing.

For small droplet radius Σ becomes of order unity and the deformation of the interface has to be accounted for. The analysis of this case is given for small and order one gas Reynolds numbers β. Two stability limits are found; on one of them the growth rate of the perturbations vanishes and on the other, which provides an upper bound for the heat flux coming from the gas to the droplet, it is imaginary, resulting in an oscillatory behavior of the perturbations.

The same analysis is applicable to a droplet of fuel burning in an oxidizing atmosphere when the stoichiometric ratio is large or the oxidizer concentration in the gas is small, so that the combustion takes place far from the droplet.

The Unperturbed State

The following description of the unperturbed droplet vaporization process is justified by the small value of the ratio of gas-to-liquid densities, that allows us to use the quasisteady approximation for the gas phase processes, and by the small value of the parameter cT_b/L, that makes the vapor pressure very sensitively dependent on the interface temperature. The effect of surface tension on phase equilibrium is neglected, retaining only its influence on the mechanical equilibrium of the interface.

In the first of the three stages mentioned in the Introduction, the vaporization rate is negligible because the interface temperature is not yet close to the boiling temperature T_b. The heat coming from the gas phase is used to heat the droplet until, after a fairly well-defined heating time, the interface temperature reaches a value that differs from T_b by a small amount of order cT_b^2/L and the vaporization begins; the temperature ceases to increase at the interface but not in the interior of the droplet, where it is lower. In a second transient period of order $t_c=\rho_L c R_o^2/k_L$, after the initiation of the vaporization, the temperature

in the bulk of the liquid is raising up to the boiling temperature. Here, ρ_L, c, and k_L are the liquid density, specific heat, and thermal conductivity, respectively, and R_o is the initial droplet radius. At the end of this second stage, the liquid temperature is nearly uniform and does not change in the rest of the vaporization. The droplet lifetime is $t_v \sim \rho_L R_o/m$, in terms of the characteristic mass flux at the interface $m \sim k_g(T_\infty - T_b)/R_o L$; k_g is the gas thermal conductivity and T_∞ the temperature far from the droplet. The droplet radius does not change appreciably in the second transient step because $t_v/t_c \sim (k_L/c)/(k_g/c_p)L/c_p(T_\infty - T_b)$ is usually large, for example $t_v/t_c \sim 8$ for a droplet of water in air at $T_\infty = 1000°K$.

In the first heating period, there is only pure conduction in the gas phase at distances of the order of the droplet radius, and the heat flux coming from the gas to the interface is given by $k_g(T_\infty - T_s)/R_o$, where T_s is the unknown instantaneous interface temperature. In the liquid, the temperature distribution is the solution of the problem

$$\frac{\partial \theta}{\partial \tau} = \frac{1}{r^2}\frac{\partial}{\partial r}\left(r^2 \frac{\partial \theta}{\partial r}\right) \tag{1}$$

$$\tau = 0: \quad \theta = 1 \tag{2}$$

$$r = 0: \quad \frac{\partial \theta}{\partial r} = 0 \tag{3}$$

$$r = 1: \quad \frac{\partial \theta}{\partial r} = -\psi_1 \tag{4}$$

where $\theta = (T - T_b)/(T_i - T_b)$ is the nondimensional liquid temperature; r is measured with the droplet radius as a unit; $\tau = t/t_c$, and $\psi_1 = (k_g/k_L)(T_\infty - T_b)/(T_b - T_i)$. A small term $-\theta k_g/k_L$ has been omitted in the right-hand side of Eq. (4) because $k_g \ll k_L$. The solution can be written in the form of a infinite series (Carslaw and Jaeger 1959) and is valid up to the instant $\tau = \tau^*$ in which $\theta(r=1) = 0$ and the vaporization begins. τ^* as a function of ψ_1 is plotted in Fig. 1a.

In the second step, the temperature and the mass fraction of the vapor in the gas are given by

$$T_{go} = T_b + (T_\infty - T_b)\frac{\exp\left[-\beta(1/r - 1)\right]}{e^{\beta} - 1} \tag{5}$$

$$Y_o = 1 - e^{-\beta Le/r} \tag{6}$$

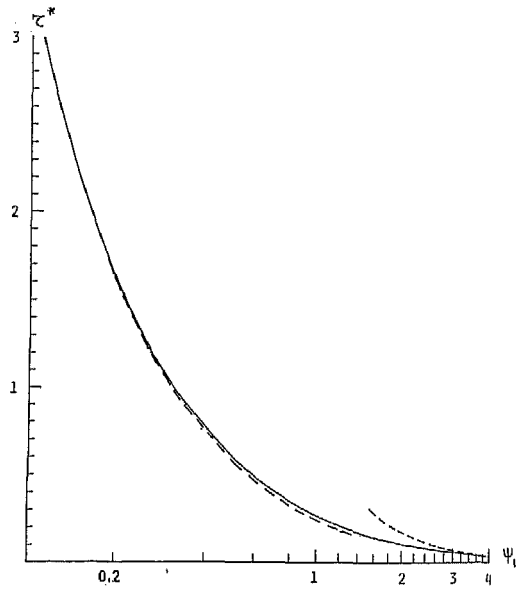

Fig. 1.a. Nondimensional time of begining of the droplet vaporization as a function of ψ_1. The dashed lines are the asymptotic expressions $\tau^* = \pi/4\psi_1^2$ and $\tau^* = 1/3\psi_1 - 1/15$ for large and small values of ψ_1.

where the subscript o is used for the basic solution and $\beta = mc_p R/k_g$ is the nondimensional vaporization rate, which is a function of τ, to be calculated as part of the solution. Le is the Lewis number of the vapor in the gas. In the liquid, the heat conduction equation (1) is still valid but the conditions (2-4) change to

$$\tau = \tau^*: \quad \theta = \theta^*(r) \tag{7}$$

$$r = 0: \quad \frac{\partial \theta}{\partial r} = 0 \tag{8}$$

$$r = 1: \quad \theta = 0 \tag{9}$$

where $\theta^*(r)$ is the temperature distribution inside the droplet at the end of the first heating step. In order to calculate $\beta(\tau)$, the additional boundary condition

$$r = 1: \quad \frac{\psi_1 \beta}{e^{\beta} - 1} = \psi_2 \beta - \frac{\partial \theta}{\partial r} \tag{10}$$

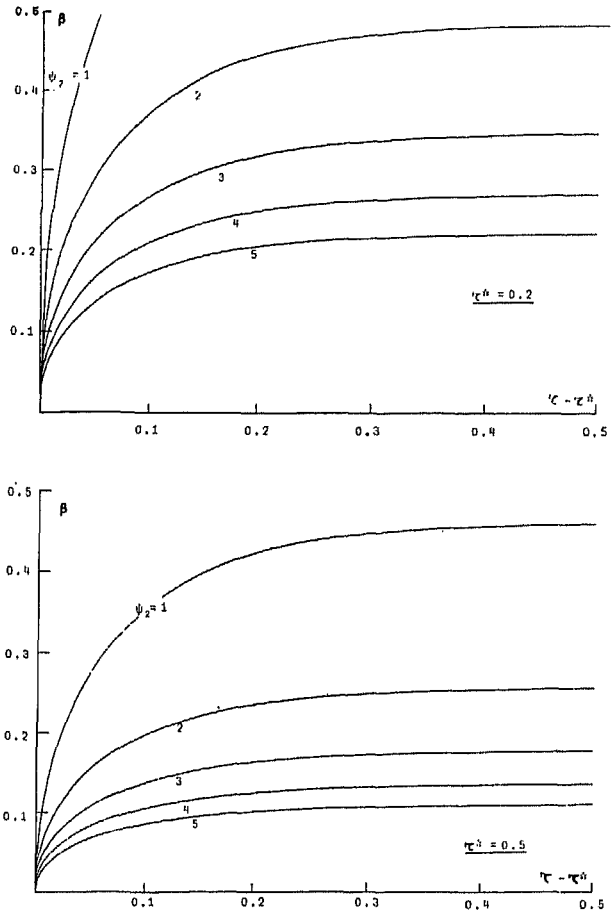

Fig. 1.b. Time evolution of the nondimensional vaporization mass flux.

is needed, where $\psi_2 = [(k_g/c_p)/(k_L/c)] \times L/c(T_b-T_i)$. Equation (10) is an energy balance through the interface. Again, the solution of Eq. (1) and Eqs. (7-9) can be written in the form of an infinite series, and the value of $\beta(\tau)$ resulting from Eq. (10) is plotted in Fig. 1b. For a detailed account of the short transition between the first and second steps see Liñán and Rodríguez (1985).

When $\tau \to \infty$, θ goes to zero and all the heat coming from the gas is used in the vaporization. The final, asymptotic value of β is

$$\beta = \beta_e = \ln[1 + c_p(T_\infty - T_b)/L] \qquad (11)$$

and this expression is also valid in the last step if the instantaneous droplet radius is used in the definition of β. The total mass flux $4\pi R^2 m$ is proportional to the droplet radius $R(t)$, whose decay follows the "R-square law"

$$\left(\frac{R(t)}{R_o}\right)^2 - 1 = 2\,\frac{L\beta_e}{c_p(T_\infty - T_b)}\,\frac{t}{t_v} \tag{12}$$

with

$$t_v = \frac{\rho_L\, c_p\, R_o^2/k_g}{c_p(T_\infty - T_b)/L}$$

Formulation of the Linear Stability Problem

The heat flux neccesary for vaporizing the liquid has to arrive from the gas counteracting the effect of the convection due to the vaporization; therefore, in the gas, the ratio of convection to conduction, measured by β, cannot be large. The characteristic Reynolds number is β/Pr and $Pr \sim 1$, so that viscosity is always important in the motion of the gas, and when the basic spherical solution is slightly perturbated, the pressure and velocity variations p_g' and u_g' are in the relation $p_g' \sim \mu_g u_g'/R$, where μ_g is the gas viscosity coefficient. On the other hand, the equilibrium of tangential stresses at the interface leads to the condition $u_L'/u_g' \sim \mu_g/\mu_L$. The ratio of viscosity coefficients is very small and the parameter $\varepsilon = \sqrt{\rho_g/\rho_L}\;\mu_L/\mu_g$ will be assumed to be of order unity. Two main simplifications result from the small value of the gas-to-liquid density ratio and the foregoing estimates. First, the time derivatives can be neglected in the gas conservation equations because they are of order $\sqrt{\rho_g/\rho_L}$ compared to the others terms in these equations. Second, the interface is nearly a fluid surface from the point of view of the liquid.

In order to estimate the characteristic time for the evolution of the perturbations, t_o, the relation $k_L T_L'/R \sim L\rho_g u_g'$, where T_L' is the temperature perturbation in the liquid, must be taken into account. This relation comes from the energy balance through the interface. The heat flux entering the liquid is always important in this balance, the basic spherical configuration being stable when it is negligible, as will be seen later. However, the liquid Prandtl number Pr_L will be assumed to be large, as is often the case so that the heat conduction in the bulk of the liquid is too slow to affect the evolution of the perturbations, except in

a thin thermal layer close to the interface, and the energy conservation equation for the liquid leads to the relation $T'_L \sim t_o u'_L (\partial T_{Lo}/\partial r)$. Carrying this to the previous relations results finally in

$$t_o \mu_L / \rho_L R^2 \sim Pr\varepsilon^2/\beta_e \tag{13}$$

The ratio $t_c/t_o \sim \beta_e Pr_L/Pr\varepsilon^2$ is large, and therefore the change in the basic unperturbated solution is negligible in the stability analysis and the normal mode method for steady basic solutions is applicable.

As a further simplification, density variations, which are due to temperature changes, are neglected in both fluids. This allows us to write the momentum equations linearized for small perturbations in terms of the pressure and the radial components of the vorticity ω_{gr} and the velocity u_{gr}, multiplying them by $\vec{x} = (r,0,0)$ after the operator $\nabla\times$ has been applied a certain number of times and the continuity equation $\vec{\nabla}\cdot\vec{v} = 0$ has been used. The result in nondimensional form is

$$\frac{\partial}{\partial t}(ru_{Lr}) = -r\frac{\partial p_L}{\partial r} + \nabla^2(ru_{Lr}) \tag{14}$$

$$\frac{\partial}{\partial t}(r\omega_{Lr}) = \nabla^2(r\omega_{Lr}) \tag{15}$$

$$\frac{\partial}{\partial t}(\nabla^2 ru_{Lr}) = \nabla^2(\nabla^2 ru_{Lr}) \tag{16}$$

for the liquid, and

$$\frac{\beta/P_r}{r^3}\left(r\frac{\partial ru_{gr}}{\partial r} - 3ru_{gr}\right) = -r\frac{\partial P_g}{\partial r} + \nabla^2(ru_{gr}) \tag{17}$$

$$\frac{\beta/P_r}{r^3}\left(r\frac{\partial r\omega_{gr}}{\partial r} + r\omega_{gr}\right) = \nabla^2(r\omega_{gr}) \tag{18}$$

$$\frac{\beta/P_r}{r^3}\left(r\frac{\partial \nabla^2 ru_{gr}}{\partial r} - \nabla^2 ru_{gr}\right) = \nabla^2(\nabla^2 ru_{gr}) \tag{19}$$

for the gas. The unprimed variables u_{gr}, p_g, u_{Lr}, and p_L are the velocity and pressure perturbations in each fluid nondi-

mensionalized with the factors m/ρ_g, $\mu_g m/\rho_g R$, $(m/\rho_L)\sqrt{\rho_L/\rho_g}$, and $(\mu_L m/\rho_L R)\sqrt{\rho_L/\rho_g}$, respectively. The time has been referred to $\rho_L R^2/\mu_L$, and r to the instantaneous droplet radius. Terms of order $\sqrt{\rho_g/\rho_L}$ corresponding to nonsteady effects in the gas and to recession of the interface in the unperturbed solution have been omitted. $r^2\omega_r$ and $r^2 u_r$ are the defining scalars for the toroidal and poloidal components of the velocity when the spherical harmonic decomposition is used (Chandrasekhar 1961).

The linearized energy conservation equations for the gas and liquid phases are

$$\alpha\beta e^{-\beta(1/r-1)}\frac{ru_{g_r}}{r^3}+\frac{\beta}{r^2}\frac{\partial T_g}{\partial r}=\nabla^2 T_g \tag{20}$$

$$\frac{\partial T_L}{\partial t}+\frac{\beta}{Pr\varepsilon}u_{L_r}\frac{\partial T_{Lo}}{\partial r}=\frac{1}{Pr_L}\nabla^2 T_L \tag{21}$$

where

$$\alpha=\frac{c_p(T_\infty-T_b)}{L}\frac{\beta}{e^\beta-1} \tag{22}$$

and the temperatures of the gas and liquid have been nondimensionalized by multiplying them by c_p/L and $c/L\delta$, respectively, with $\delta=(k_g/c_p)/(k_L/c)$. Notice the difference with the previous section.

The mass conservation equation for the vaporizing species in the gas can be obtained from Eq. (20) by replacing β by βLe and α by $-\beta$Le.

As the unperturbed solution is quasisteady and normal modes are used, the time dependence is exponential for every variable. In addition, the dependence on the angular variables is accounted for with the spherical harmonic decomposition, and the gas velocity and interface deformation, for example, are written as the real parts of $u_{gr}(r,\theta,\psi,t) = u_{gr}(r)\exp(\Omega t)Y_l^n(\theta,\psi)$ and $r_s-1=\chi\exp(\Omega t)Y_l^n(\theta,\psi)$, respectively, where the deformation has been referred to the droplet radius. The same name is used for a variable and for its radial part. l and n are integers defining the angular mode. As a consequence of the symmetry of the basic solution, n does not appear in the results and Ω, which is a complex number in general, depends only on l and the parameters. The equations for the radial functions result from Eqs. (14-21), replacing $\partial/\partial t$ by Ω and ∇^2 by $1/r^2 d/dr(r^2 d/dr)-l(l+1)/r^2$.

In addition to the regularity conditions at the origin and at infinity, the solutions of these equations are subject to the following continuity and conservation conditions at the interface, written for the radial part of the variables at $r = 1$.

$$(\beta/\varepsilon Pr)u_{L_r} = \Omega\chi \tag{23}$$

$$\varepsilon\left[p_L - 2\frac{du_{L_r}}{dr}\right] = p_g + 2\frac{\beta}{Pr}(u_{g_r} - \chi) - 2\left[\frac{du_{g_r}}{dr} + 6\chi\right]$$

$$+(l-1)(l+2)\Sigma\chi + M(Y - \beta Le\chi) \tag{24}$$

$$\frac{d}{dr}\frac{r^2 u_{g_r}}{l(l+1)} + \chi = 0 \tag{25}$$

$$r^2\omega_{g_r} = 0 \tag{26}$$

$$\varepsilon\left[\frac{d^2}{dr^2} + l(l+1) - 2\right]\frac{ru_{L_r}}{l(l+1)} = \left[\frac{d^2}{dr^2} + l(l+1) - 2\right]\frac{ru_{g_r}}{l(l+1)} - 4\chi$$

$$+ M(Y - \beta Le\chi) \tag{27}$$

$$\frac{d}{dr}(\omega_{L_r} - \omega_{g_r}) = 0 \tag{28}$$

$$T_g + \alpha\chi = 0 \tag{29a}$$

$$T_L + \frac{\partial T_{Lo}}{\partial r}\chi = A(Y - \beta Le\chi) \tag{29b}$$

$$\beta u_{g_r} + \frac{dT_L}{dr} = \frac{dT_g}{dr} + \alpha\beta\chi \tag{30}$$

$$\beta Le\, e^{-\beta Le}\, u_{g_r} - \beta LeY + \frac{dY}{dr} = 0 \tag{31}$$

where terms of order $\sqrt{\rho_g/\rho_L}$ have been neglected, as well as a small term $\chi\partial T_{Lo}/\partial\tau$ in the left-hand side of Eq. (30). Equation (23) is the mass conservation condition. Equation (24) is the momentum conservation condition, the convective flux being negligible in the liquid. $\Sigma = \rho_g\sigma/m\mu_g$ is the nondimensional surface tension coefficient and $M = (R_g T_b^2/LY_o) \times$ $\times \rho_g(d\sigma/dT)/m\mu_g < 0$, where R_g is the vapor constant, is a

Marangoni number. The conditions of continuity of tangential velocities at the interface and the balance of tangential stresses lead to Eqs. (25,26) and (27,28), taking into account the continuity equation. The last term in Eq. (27) is the tangential stress due to the change of surface tension with the temperature, which, in turn, is related to the local concentration of the vapor at the interface through the equilibrium condition. $A = R_g c T_b^2 / L^2 Y_o(1)\delta$, appearing in the linearized equilibrium condition (29b), gives the magnitude of the interface temperature changes on the liquid-vapor saturation curve. Notice that these temperature changes are neglected in Eq. (29a) because they are small compared to the temperature perturbations in the gas. Finally Eqs. (30) and (31) come from energy and mass balance through the interface.

The equations set (15), (18), (26), and (28), with the regularity conditions at the center of the droplet and at infinity, has the trivial solution $\omega_{gr} = \omega_{Lr} = 0$. Only the other equations are going to be considered from here on.

Perturbations Without Deformation of the Interface

The normal stress due to the surface tension is proportional to $1/R$, whereas the normal viscous stress of the gas on the interface varies like $1/R^2$ because it arises from a velocity gradient and the velocity itself varies like $1/R$. Σ is a measure of the relative importance of both effects and it is proportional to the droplet radius ($m \sim 1/R$); therefore, the larger the droplet size, the more difficult it is to deform the interface by the action of perturbations due to local changes in the vaporization rate. Here we consider the limit $\Sigma \gg 1$, which is appropriate for all but very small droplets, neglecting the deformation of the interface. In addition, it will be assumed that $\beta_e \ll 1$ (always with $\beta_e Pr_L \gg 1$), so that viscosity dominates the motion of both fluids and the left-hand sides of Eqs. (14-19) can be neglected. The velocity and pressure perturbations in the gas and liquid phases can be written as

$$u_{gr} = \frac{-c_l}{2(2l-1)r^l} + \frac{b_l}{r^{l+2}} \qquad p_g = -\frac{c_l}{(l+1)r^{l+1}}$$

$$u_{Lr} = \frac{B_l r^{l+1}}{2(2l+3)} + C_l r^{l-1} \qquad p_L = \frac{B_l r^l}{l} \tag{32}$$

whereas the temperature and concentration perturbations are given by

$$T_g = \frac{\alpha\beta}{r^l}\left(1-\frac{1}{r}\right)\left(\frac{c_l}{4l(2l-1)}-\frac{b_l}{2(l+1)r}\right) \tag{33}$$

$$Y = \frac{\beta Le}{l+1}\left(-\frac{c_l}{2(2l-1)}+b_l\right)\frac{1}{r^{l+1}}+O(\beta^2) \tag{34}$$

$$T_L = -\frac{\beta}{\varepsilon Pr\Omega}\frac{\partial T_{Lo}}{\partial r}\left(\frac{B_l r^{l+1}}{2(2l+3)}+C_l r^{l-1}\right)+AY(1)\exp\left(\sqrt{\Omega Pr_L}\,(r-1)\right) \tag{35}$$

where use has been made of Eqs. (29) and (31). The last term in Eq. (35) is due to the temperature changes at the interface and is associated with the thin thermal layer close to it. Carrying these results to conditions (23), (25), (27), and (30) at the interface, the system

$$\frac{B_l}{2(2l+3)}+C_l=0 \tag{36a}$$

$$c_l\frac{l-2}{2(2l-1)}-b_l l=0 \tag{36b}$$

$$\varepsilon\left(B_l\frac{l(l+2)}{2l+3}+C_l 2(l^2-1)\right)=-c_l\frac{l^2-1}{2l-1}+b_l 2l(l+2)+MY(1)l(l+1) \tag{36c}$$

$$-\frac{\beta}{\varepsilon Pr\Omega}\frac{\partial T_{Lo}}{\partial r}\bigg|_1\left(B_l\frac{l-1}{2(2l+3)}+C_l(l-3)\right)+A\sqrt{\Omega Pr_L}\,Y(1)$$

$$+\beta\left(-\frac{c_l}{2(2l-1)}+b_l\right)=0 \tag{36d}$$

is obtained. The last equation comes from Eq. (30); the perturbation in the heat flux from the gas to the interface drops out because it is of order β compared to the others terms in this equation. The system (36) leads to the dispersion relation

$$\Omega=\frac{(\alpha-\beta)(3+M\beta Le)l(l+1)}{\varepsilon^2 Pr(2l+1)(l+1+ALe\sqrt{\Omega Pr_L})}\,,\qquad l\geq 2 \tag{37}$$

where use has been made of the result $\partial T_{Lo}/\partial r\,|_1=\alpha-\beta$. When $cT_b/L\to 0$, both A and M vanish and the interface temperature does not change. In this case, the basic configuration is unstable. The reason is that below the interface regions

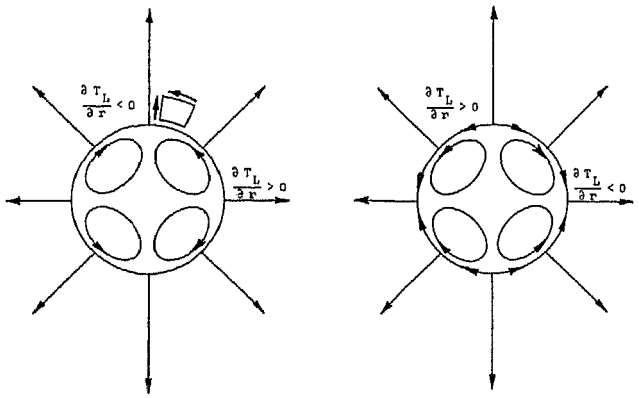

Fig. 2. Schematic representation of the viscous stresses and Marangoni effects in the case $\Sigma \gg 1$, $\beta_e \ll 1$.

where the mass flux increases ——— that is, where $Y_1^n(\theta,\psi) < 0$ if it is chosen $c_1 > 0$, because $u_{gr}(r=1) = -c_1 Y_1^n/l(2l-1)$ ——— the radial velocity in the liquid is directed toward the center of the droplet (for $r < 1$, the radial velocity is dominated by the component $C_1 r^{l-1} Y_1^n(\theta,\psi)$ and $C_1 = 3(c_1/\varepsilon)/2(4l^2-1) > 0$). The temperature of every liquid particle does not change due to the perturbations because the heat conduction is negligible in the bulk of the liquid, and therefore the heat flux entering the droplet decreases at these regions of the interface and increases where $u_{gr}(r=1) < 0$. There is more energy available for vaporization where initially $u_{gr} > 0$ than where $u_{gr} < 0$, and, as shown in the result (37) with $A = M = 0$, the differences in the local vaporization rate increase even more, (see Fig. 2a).

The interface temperature changes, when cT_b/L is different from zero, are reflected in the denominator of Eq. (37). Their effect is not able by itself to stabilize the spherical configuration, but the temperature changes also lead to changes in surface tension whose effect is the term proportional to M in Eq. (37), which is stabilizing for the usual case $M < 0$. At the interface regions where the vaporization rate increases, $u_{gr} > 0$, the vapor mass fraction Y and the temperature also increase, leading to a decrease in surface tension; then the liquid is dragged along the interface toward the colder regions, being replaced by cold liquid coming from the interior of the droplet, (see Fig. 2b). This

liquid motion due to Marangoni effects increases the heat flux toward the liquid side at these hot interface regions.

The basic configuration will be stable when the stabilizing Marangoni effects prevail over destabilizing effects due to viscous stresses.

The previously discused effects are proportional to $\partial T_{Lo}/\partial r|_1$, and, therefore, the growth rate of the perturbations decreases with time due to the time evolution of the basic state. For values of $\beta_e Pr_L \sim 1$ the response time of the perturbations equals the characteristic time of the basic solution and the previous normal mode analysis ceases to be valid. However $\beta_e Pr_L \sim 1$ can be understood as a qualitative criterion for stability, taking into account that in this case there is not time enough for the growth of the perturbations.

Perturbations with Deformation of the Interface

When the droplet is small enough, Σ is not large compared to unity and the effect of surface tension is not able to keep the interface spherical, so that its deformation has to be accounted for in the analysis. Notice that $\Sigma \sim 1$ for a water droplet of a few microns with $\beta \sim 1$.

We begin by analysing the effects of the surface deformation for $\Sigma \sim 1$ in the case of small values of β_e (with $\beta_e Pr_L >> 1$). Afterward the analysis is extended to order one gas Reynolds number but for simplicity we will consider here the limiting case $cT_b/L \to 0$, so that $A = M = 0$ and therefore, in particular, the Marangoni effects are excluded. The velocity and pressure perturbations are still given by Eq. (32), but new terms, proportional to the interface deformation χ, have to be included in the right-hand sides of the conditions (36) at the interface; these terms are $(\varepsilon Pr/\beta)\Omega\chi$ in Eq. (36a), $-l(l+1)\chi$ in Eq. (36b), and $-4l(l+1)\chi$ in Eq. (36c). An additional relation, to determining χ, comes from the normal momentum conservation condition through the interface (24), which can be written as

$$-\varepsilon\left(B_l \frac{l^2-l-3}{l(2l+3)} + 2(l-1)C_l\right) = -c_l \frac{l^2+3l-1}{(l+1)(2l-1)} + 2(l+2)b_l - 12\chi + (l-1)(l+2)\Sigma\chi + MY(1) \qquad (36e)$$

The deformation of the interface induces a temperature perturbation in the gas phase given by $T_g = -\alpha\chi/r^{l+1}$, which is much greater than that in Eq. (33), and a new term $-\alpha(l+1)\chi$ appears in the right-hand side of Eq. (36d). The modified

set of equations, with Eq. (36e) included, leads to the dispersion relation

$$A\Omega_1^2 + B\Omega_1 + C = 0 \tag{38}$$

where

$$A = 2\,\frac{l^2+4l+3}{l^2}\,\frac{1+A\mathrm{Le}\sqrt{\mathrm{Pr}_L\Omega}/(l+1)}{\alpha/\beta-1}$$

$$B = \left\{\frac{(2l+1)(l+2)}{l}\,\Sigma+4\,\frac{l^3+2l^2-4l-2}{l(l-1)}\right\}\frac{1+A\mathrm{Le}\sqrt{\mathrm{Pr}_L\Omega}/(l+1)}{\alpha/\beta-1}$$

$$+2\,\frac{2l^3-8l-9-M\beta\mathrm{Le}(l^2+3l+3)}{l(l+1)}$$

$$C = 2\,\frac{2l^3-5l+12-M\beta\mathrm{Le}(l^2+2l-4)}{l-1} - (3+M\beta\mathrm{Le})(l+2)X$$

and $\Omega_1 = \varepsilon^2\mathrm{Pr}\Omega/\beta$.

The basic state is seen to be stable when the temperature of the liquid is uniform, $\alpha = \beta$. In this case $c_1 = 0$ and the normal stress of the gas on the interface has a restoring effect, like the surface tension. When $(\alpha-\beta)/\beta \sim 1/\mathrm{Pr}_L \ll 1$ the time evolution of the perturbations become very slow and the normal mode analysis is not applicable.

The modes $l=1$ are associated with translations of the droplet without deformation of the interface. Only Marangoni effects can limit the growth of these perturbations, when $-M\beta\mathrm{Le} > 9$. The discussion that follows for the other modes is restricted to the case $A = 0$, so that perturbations in the interface temperature appear only through their effect on the surface tension. Eq. (38) becomes a quadratic expression and the stability limits can be obtained by equating to zero the coefficients of the different powers of Ω_1. The limit with $\Omega_1 = 0$ is given by

$$\Sigma = \frac{2}{3}\,\frac{2l^3-5l+12-(l^2+2l-4)M\beta\mathrm{Le}}{(l-1)(l+2)(1+M\beta\mathrm{Le}/3)} \tag{39}$$

The minimum value of the right-hand side for l integer is obtained for $l=2$. These modes are the first to lose stability and the basic state is unstable for $\Sigma > (3 - 2M\beta\mathrm{Le}/3)/(1 + M\beta\mathrm{Le}/3)$. When $-M\beta\mathrm{Le} > 3$ the stability limit dissappears and every perturbation decreases with time.

The stability limit with Ω_1 imaginary is obtained from (38) by equating to zero the coefficient of the linear term in Ω_1. With $\alpha/\beta > 1$, the result is meaningful only for $l=2$, because greater values of l lead to $\Sigma < 0$ on the stability limit. There are five modes with $l=2$, and for these the stability limit is

$$\frac{\alpha-\beta}{\beta} = \frac{2}{3}\,\frac{6+5\Sigma}{1+13M\beta Le/9} \tag{40}$$

which gives an upper bound to the nondimensional heat flux coming from the gas, α. This limit moves to infinity and disappears for $-M\beta Le = 9/13$; only the previous limit, with $\Omega_1 = 0$, remains for $9/13 < -M\beta Le < 3$.

The results (39) and (40) are plotted in Fig. 3, as boundaries of the stability domain of the basic solution.

As can be easily seen from the previous equations, the velocity and pressure perturbations in the liquid vanish when $\Omega_1 = 0$. The perturbations of pressure and normal viscous stress of the gas on the interface are positive in the regions where $\chi < 0$, and negative where $\chi > 0$, whereas the ef-

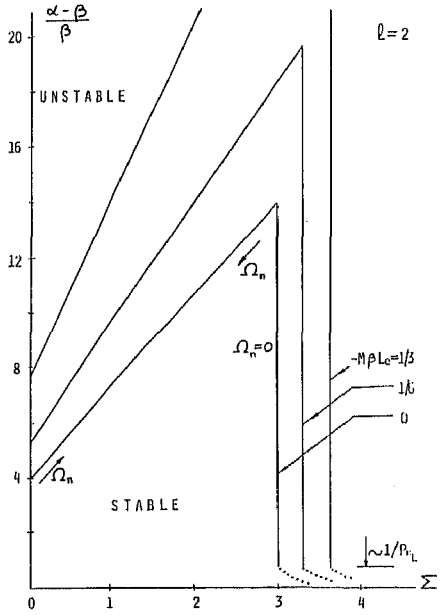

Fig. 3. Stability region for $1 >> \beta_e >> 1/Pr_L$ and several values of $-M\beta Le$. The arrows indicate the direction of increase of the frequency on the stability limit. When $(\alpha - \beta) \sim 1/Pr_L$ the normal mode analysis fails and this is represented by the dotted lines.

fect of the surface tension is opposite. Therefore the equilibrium is possible only for a value of Σ, given by Eq. (39). It is also easy to compute the small perturbations in the pressure and normal stress of both fluids on the interface close to this stability limit, leading to the result

$$\Omega_1 = \frac{(\alpha/\beta-1)12\Sigma'}{15-\alpha/\beta} \quad \text{for} \quad \Sigma' = (\Sigma-3) \ll 1 \quad \text{and} \quad M = 0 \qquad (41)$$

so that the perturbations grow if Σ is greater than 3, at least while $0 < (\alpha/\beta-1) < 14$, which is the range of interest (see Fig. 3).

The second stability limit, with Ω_1 imaginary, is associated with the existence of a term quadratic in Ω_1 in Eq. (38). This derives from the fact that the velocity perturbations are proportional to both the interface deformation and its velocity, whereas the perturbation in the heat flux entering the liquid, which, together with the heat flux coming from the gas, determines the local vaporization rate, is proportional to the integral of the velocity, generating a term $1/\Omega_1$ in Eq. (36d).

The analysis can be extended to see how both stability limits change when β_e grows to values of order unity. According to the estimates in the section on formulation, the time derivatives can no longer be neglected in the momentum equations for the liquid, Eqs. (14-16), but the solutions of these equations can be written in terms of modified Bessel functions. The left-hand sides of Eqs. (17-19) must also be retained; the solutions of these equations must be obtained numerically. Carrying them and the solutions of Eqs. (20,21) to the boundary conditions (23-30), an homogeneous system of linear equations results; the compatibility condition provides the dispersion relation between Ω and 1, with the seven parameters α, β, Pr, Σ, ε, A, and M. This will not be written for the sake of brevity. The following results correspond to the limiting case of constant interface temperature, so that $A = M = 0$.

The stability limit with Ω imaginary is obtained by putting $\Omega = i\Omega_n$ in this dispersion relation. The result for Pr = = 0.7, $\varepsilon = 1$, and several values of β is plotted in Fig. 4. Also plotted in this figure is the stability limit with $\Omega=0$, which does not depends on α. Like in the case $\beta_e \ll 1$, the perturbations in the liquid vanish on this stability limit, but now we find also perturbations in the flux of momentum with the same direction as the perturbations in the pressure and normal viscous stress of the gas on the interface; such perturbations have to be balanced by the surface tension.

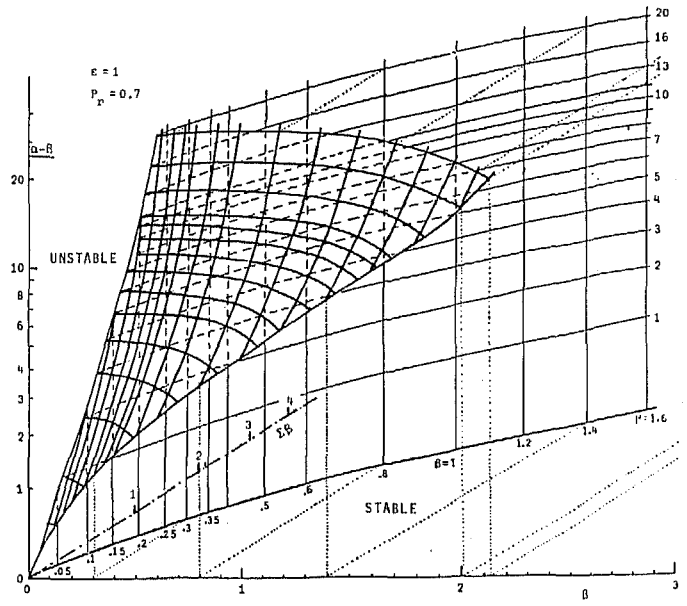

Fig. 4. Stability limits for $\Sigma \sim 1$. On the vertical axis $\alpha-\beta$ is the instantaneous heat flux entering the liquid. The vertical surface is the stability limit with $\Omega = 0$ and the stability region is ahead this vertical surface and below the inclined one. It is $\Sigma\beta = \sigma Re_p \rho_g / \mu_g k_g$.

The two stability limits enclose the region, extending to infinity in some parts, where the basic state is stable. The plot in Fig. 4 corresponds to $l = 2$, as this is the critical value of l for the most unstable perturbations. There are five different angular functions for $l = 2$ ($n = -2$ to 2), the degeneracy being associated with the symmetry of the unperturbated solution. Two maxima and two minima appear in the deformation of the interface, so that, when unstable, the droplet is likely to slipt into two parts.

There is a region of thickness $1/Pr_L$ around the surface $\Omega = 0$ in Fig. 4 (and also around the vertical line in Fig. 3), in which $\Omega \sim 1/Pr_L$ and the normal mode method fails. This region widens when $(\alpha-\beta)$ decreases and for $(\alpha-\beta) \sim 1/Pr_L$, is $\Omega \sim 1/Pr_L$ everywhere. In the stability analysis, the unsteady effects become negligible in the liquid momentum equations, and the problem can be reformulated in terms of $T_L(r,t)$ and $X(t)$ only, but the generality of the normal mode method is lost. The situation is similar, but simpler, for $\beta \sim 1/Pr_L$. If $\alpha = \beta$ there is not heat flux toward the liquid from the interface and the spherical solution is stable, as mentioned before.

Concluding Remarks

The analysis carried out in this paper shows the existence of instabilities of the droplet vaporization process in a stagnant atmosphere that may appear during the early stage of the vaporization, when the temperature within the droplet is not yet uniform. These instabilities are due to the motion of the liquid toward the interior of the droplet in those regions where the surface temperature, and therefore the vaporization rate, is higher; the liquid motion is induced by the gas phase viscous stress.

The destabilizing effects of the viscous stresses are stronger for $\Sigma \gg 1$, when the effects of the surface tension forces are capable to maintain the droplet spherical, counteracting the deforming effects of viscous stresses, so as to impede the deformation of the droplet. This is the case for large droplet radius.

The analysis of the strong vaporization case, involving values of $\beta \sim 1$, should be extended to include the Marangoni effects that have been found to be stabilizing in the simplified analysis carried for $\beta_e \ll 1$.

It should also be noticed that the characteristic growth time of these instabilities, associated with the temperature nonuniformity within the droplet, becomes very large when the temperature gradients in the liquid tend to zero, in the last long stage of the droplet history, and these instabilities cease to be important.

During the droplet lifetime the representative point of the quasisteady state in the parameter space in Fig. 4 changes. Early during the second stage $\beta \ll 1$, while α and $\Sigma\beta = \sigma \mathrm{Re}_p \rho_g / \mu_g k_g$ are finite, so that the spherically symmetrical state appears as unstable. However, the characteristic time of the perturbations is $\beta \mathrm{Pr}_L$ times shorter than the characteristic time t_c for change in β; so that at early times when β is small the perturbations grow very slowly unless $\beta \mathrm{Pr}_L \gg 1$. For liquids with nor very large values of Pr_L, β will grow, taking the system to the stable region in Fig. 4, before the perturbations grow significantly.

As mentioned in the Introduction, there are no instabilities associated to nonsteady effects in the gas phase. Although the analysis is not presented in the text, it is easy to understand this result when $\beta_e \ll 1$ and radial convection effects are negligible. In this case the temperature perturbations in the gas are due mainly to deformations of the interface, which are very small, so that the changes in the heat flux toward the interface are not strong enough to modify the local mass vaporization rate; the resulting linearized problem is the same as that for a constant-volume bub-

ble in a viscous fluid, which leads to a stable behavior, (Lamb 1932, Chandrasekhar 1961, Reid 1969). Numerical results for the corresponding eigenvalue problem show the same decaying behavior of the perturbations even for large values of the Reynolds number, when $\beta_e \sim 1$.

The reader should remember that the analysis given here does not include the effect of the motion of the droplet with respect to the enviroment, based on the assumption that the corresponding Reynolds number is small compared with unity.

The analysis can be extended to account for the linear transient response of the liquid phase in the burning of a fuel droplet whose vapor reacts with an oxidizer present in the atmosphere, leading to a diffusion controlled flame in the gas phase. The results (see Higuera 1985) are very similar to the ones of this paper and both coincide exactly, as mentioned in the Introduction, in the limiting cases when the flame sheet lies far from the droplet, and also when $\beta_e \ll 1$, or when the Lewis number of the fuel vapor and the oxidizer are equal to each other, or one of them is equal to the unity.

Acknowledgment

Partial support for this research by the Spanish CAICYT under Project 2291083 is acknowledged.

References

Carslaw, H.S. and Jaeger, J.C. (1959) Conduction of Heat in Solids, 2nd ed. Oxford University Press, New York.

Chandrasekhar, S. (1959) The oscillations of a viscous liquid globe. Proc. London Math. Soc. 9(3), 141-149.

Chandrasekhar, S. (1961) Hydrodynamic and Hydromagnetic Stability. Clarendon Press, Oxford (reprinted by Dover, New York, 1981).

Hickman, K.C.D. (1952) Surface behaviour in the pot still. Indust. Engng. Chem. 44(10), 1892-1902.

Hickman, K.C.D. (1972) Torpid phenomena in pump oils. J. Vac. Sci. Techn. 9(10), 960-976.

Higuera, F.J. (1985) Estabilidad de la Combustión de Propulsantes Condensados, Ph.D. Thesis, Universidad Politécnica de Madrid, Spain.

Lord Kelvin (1980) Oscillations of a liquid sphere. Mathematical and Physical Papers, Vol. 3, pp. 384-386. Clay and Sons, London.

Lamb, H. (1932) Hydrodynamics, 6th ed. Cambridge University Press, Cambridge, England (reprinted by Dover, New York, 1945).

Landau, L.D. (1944) On the theory of slow combustion. Acta Phys. Chem. 19(1), 77-85.

Langmuir, I. (1918) The evaporation of small spheres. Phys. Rev. 12(5), 368-370.

Liñán, A. and Rodríguez, M. (1985) Droplet vaporization, ignition and combustion. Proc. 1st Colloque on Combustion in Thermal Engines, Madrid, Spain, pp. 10/0-10/22.

Palmer, H.J. (1976) The hydrodynamic stability of a rapidly evaporating liquid at reduced pressure. J. Fluid Mech. 75(3), 487-511.

Lord Rayleigh (1894) The Theory of Sound, 2nd ed., Vol. 2, p. 371. MacMillan, London (reprinted by Dover, New York, 1945).

Reid, W.H. (1960) The oscillations of a viscous liquid drop. J. Appl. Math. 18(2), 86-89.